Dynamic Behavior of Cable Supported Bridges Affected by Corrosion Mechanisms under Moving Loads

Lonetti P., Pascuzzo A., Sarubbo R.
Department of Structural Engineering, University of Calabria, Via P. Bucci, Cubo39-B, 87030, Rende, Cosenza, Italy
email: lonetti@unical.it; apascuzzo@unical.it; raffaele.sarubbo@gmail.com;

Abstract: The dynamic behavior of cable supported bridges subjected to moving loads and affected by corrosion mechanisms in the cable suspension system is investigated. A generalized formulation based on the finite element method is developed, in which both in-plane and out-of plane deformation modes have been considered in the dynamic behavior of the bridge. Moreover, local vibration effects of the cable elements and large deformations are taken into account by reproducing geometric non-linearities involved in the cable system, the girder and pylons. The cable corrosion mechanisms, which essentially determine a reduction of the cable stiffness, are formulated consistently with a theoretical formulation based on Continuous Damage Mechanics (CDM). Numerical results in terms of time histories of typical kinematic and stress design variables for cable-stayed and suspension bridges are reported by means of comparisons between damaged and undamaged bridge configurations.

Keywords: Cable Supported Bridges, Corrosion, Finite Element Method, CDM.

1. Introduction

The dynamic behavior of cable supported bridges subjected to moving loads and affected by corrosion mechanisms in the cable suspension system is investigated.

Cable supported bridges strongly depend on the cable system, which can be defined according with suspension or cable-stayed cable configurations. The former comprises a parabolic profile of the main cable and vertical hanger cables connecting the stiffening girder to the main cable; the latter consists of straight cables connecting the stiffening girder to the pylon [1]. Both cable systems are frequently employed in the context of long spans, leading to slender and flexible structures, in which, typically, the dead loads are comparable with those involved in the live load configuration.

During their life, cable supported bridges are affected by several damage phenomena, which produce a reduction of the mechanical properties of the bridge constituents. As a matter of fact, the cable system usually consists of high tensile galvanized steel wires, which are frequently exposed to severe environmental conditions such as marine environment, rain, pollution, ect. Such phenomena lead to degradation effects, which may cause a reduction of the stiffness properties or, in extreme cases, the complete failure of a single or multiple cable elements [2 – 3].

Old suspension bridges often suffer from the onset of deteriorated cables. Actually, experimental observations on existing bridge structures have shown the presence of damage mechanisms on the steel wires of the main-cable, which typically are affected by severe corrosion phenomena or, in the extreme case, by the complete fracture of the wires [4]. Furthermore, the vibrations induced by moving loads can cause the deterioration of the cables according to the known phenomenon of the "fretting-fatigue corrosion". Therefore, corrosion mechanisms involve a gradual loss of structural performance as well as of the structural security making the structure more sensitive to the effects of the moving load.

To this end, it is necessary for design purposes to check the safety of the structure and its robustness against corrosion mechanisms under the action of moving loads.

A brief literature review reveals that the problem of moving loads for cable supported bridges was mainly analyzed for undamaged bridge structures. In this framework, the bridge behavior was analyzed by means of finite element models, in which local vibration effects of the cable elements were taken properly into account [5 - 6]. In particular, for slender and flexible structures several studies on supported bridges have denoted that it is necessary to take into account the influence of the external mass and its motion and thus introducing an accurate description of the inertial forces arising from the bridge deformations and moving load kinematic. At this aim, Bruno et al. [7–9] have proved that the external loads were able to produce high amplifications of the main bridge kinematic and stress design parameters, leading to non-standard excitation modes in the bridge structure.

On the other hand, few studies were made on the influence of cable corrosion mechanisms on the dynamic behavior of bridges. As a matter of fact, Lepidi et all. [10] have analyzed from the static and dynamic points of view, the effect of the damage mechanisms on single cable element in terms of intensity, extent and position. Starting from Lepidi's model for damaged suspended cables, Materazzi and Ubertini [11] have presented a mathematical formulation to analyze the vertical vibration of suspension bridges with a damage in the main cables. In this framework, a parametric analysis with the purpose of investigating the sensitivity of natural frequencies and mode shapes to damage is proposed. However, further investigations to verify code prescriptions and to quantify the influence on the bridge behavior of the dynamic excitation produced by the damage characteristics of the cable system are much required.

The purpose of this study is to investigate the influence on cable supported bridge structures of corrosion mechanisms in the cable-stayed and suspension systems. To this end, a parametric study for cable-stayed and suspension bridges was considered to analyze the dynamic behavior of both damaged and undamaged bridge structures under the application of moving loads.

2. Theoretical Formulation

The dynamic behavior of cable supported bridges was analyzed by using a generalized formulation based on the finite element method in which both in-plane and out-of plane deformation modes have been accounted for. Moreover, local vibrations of the cable elements was taken into account by reproducing the non-linearities involved in the cable-sag effect in the cable system as well as large deformations in the girder and the pylons.

2.1 Cable formulation

The cable element is based on a 3D nonlinear geometric formulation. The theoretical formulation is consistent with large deformation theory based on Green-Lagrange's strain measure and the second Piola-Kirchhoff stress, whereas the material behavior is assumed to be linearly elastic. The weak form can be derived by using the principle of D'Alembert as follows:

$$\begin{aligned} &\sum_c \int \sigma_n \delta\varepsilon_n dV_0 + \sum_c \int \mu_c \ddot{\underset{\sim}{u}} \delta \underset{\sim}{u} dV_0 = \\ &\sum_c \int \underset{\sim}{g}_c \delta \underset{\sim}{u} dV_0 + \sum_c \underset{\sim}{F} \delta \underset{\sim}{u} dV_0 \end{aligned} \tag{1}$$

where $\sum(.)$ involves a summation over the elements introduced to discretize the geometry of the cable, the dot represents the time derivative with respect to the time, $\underset{\sim}{u}$ is the displacement vector, μ_c is the mass per unit volume cable density, g_c is the self-weight load of the cable and F is reaction force vector.

2.1.1 Initial configuration under dead loads

The cable behavior is mostly influenced by the preexisting stress and strain status so the initial configuration under the dead loading must be identified. The values of the cable tensions were obtained enforcing the deck to stay in the undeformed configuration during the application of the dead loads, by means of the following conditions [1]:

$$\underset{\sim}{u}_z^G + \underset{\sim}{C} \cdot \underset{\sim}{X} = 0 \tag{2}$$

where $u^G{}_z$ is a vector containing the self-weight displacements in absence of the pre-stressing forces, $\underset{\sim}{X}$ is the internal stress in the cable system, C is the flexibility matrix of the structure.

It is worth noting that since the structure is characterized by a nonlinear behavior, Eq. (2) corresponds to a nonlinear equation system, whose solution requires a numerical procedure to be calculated. To this end, an incremental iterative procedure to compute the internal force vector, by means of an optimization solving problem have been developed.

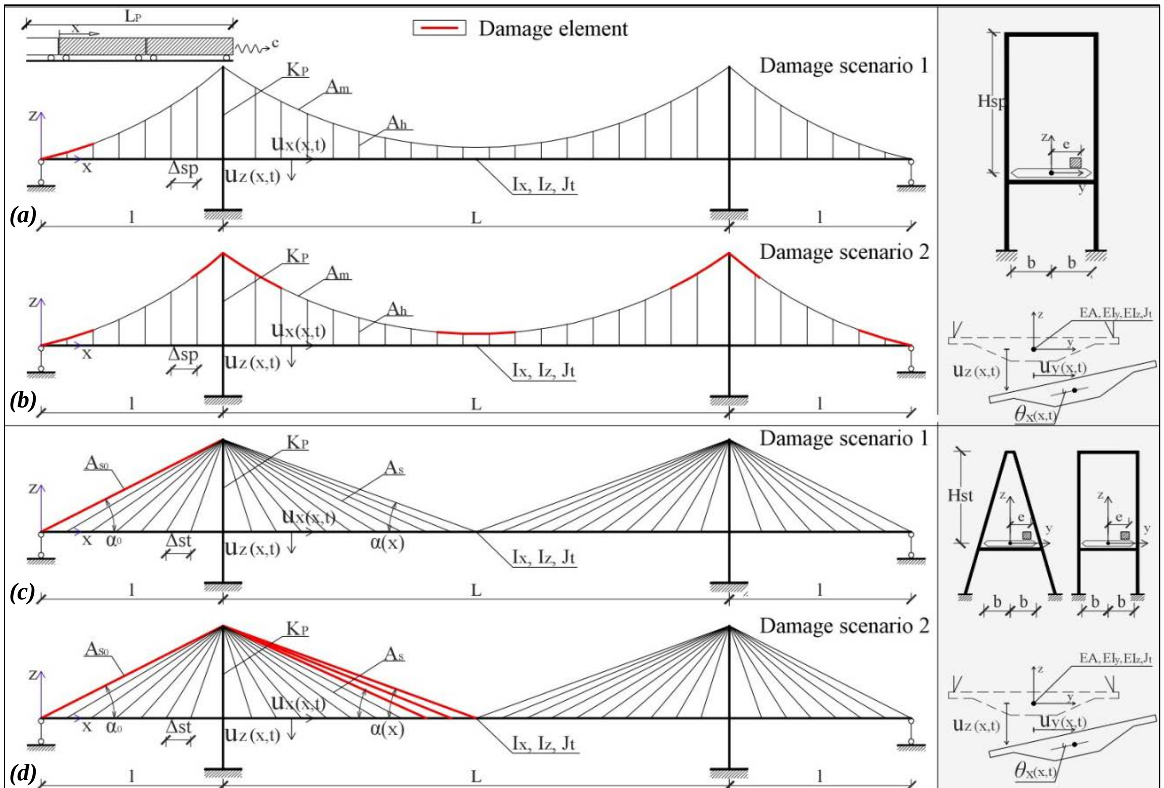

L= 1050 m; l= 350 m; H_{sp}= 168 m; H_{st}= 210 m; b= 10 m; Δ_{st}= 10 m; Δ_{sp}= 20 m; L_p= 1050 m; e= 5 m;
g= 30000 kg/m; A= 9.54 m^2; σ_g= 3.58E8 Pa; A_m= 0.488 m^2; A_h= 0.0106 m^2; A_{s0}= 0.248 m^2; A_s= g $\Delta_{st}/(\sigma_g \sin\alpha)$;
I_y= 3.057 m^4; I_z= 113.11 m^4; J_t= 1.0332 m^4; p= 30000 kg/m; E= 2.06E11 Pa; K_p= 7357500 N/m;

Figure 1. Structural model of the bridge, damage scenarios and bridge properties utilized in the results.

2. Girder formulation

The girder and tower are described by 3D geometric nonlinear beam elements, based on an Euler-Bernoulli (EB) formulation and Green-Lagrange's strain assumption. The girder is connected with the cable elements at the end points of the cross-section on the *yz* plane. With reference to Fig.1, the displacements of the cross-section are expressed by the following relationships.

$$\bar{u}_x = u_x - \vartheta_z y,\ \ \bar{u}_y = u_y,\ \ \bar{u}_z = u_z + \vartheta_x y \qquad (3)$$

where (u_x, u_y, u_z) and (θ_x, θ_y, θ_z) are the displacements and rotation fields of the centroid axis of the girder with respect to the global reference system, respectively. The external loads are assumed to proceed, with constant speed *c* from left to right along the bridge development and are supposed to be located, eccentrically with respect to the geometric axis of the girder. In the proposed modeling the moving load is considered to be perfectly connected to the girder profile, neglecting any frictional forces of the suspension system of the external loads or the roughness effects produced by girder profile. As a result, the cinematic parameters of the moving system coincided with the ones defined by the girder. This assumption is quite consistent in the framework of cable supported bridges with long spans, in which, typically, such interaction forces produced by localized dynamic effects are negligible with respect to the global bridge vibration. However, the interaction between moving loads and bridge motion was considered introducing non-standard contributions arising from Coriolis and centripetal inertial forces, which are, mainly, produced by the coupling behavior between moving system and bridge deformations. In particular, with respect to a fixed reference system, velocity and acceleration functions of the moving system were evaluated by means of a Eulerian description, as:

$$\dot{\bar{u}}_z=\frac{\partial\bar{u}_z}{\partial t}+\frac{\partial\bar{u}_z}{\partial x}c,$$
$$\ddot{\bar{u}}_z=\frac{\partial^2\bar{u}_z}{\partial t^2}+\frac{\partial^2\bar{u}_z}{\partial x\partial t}2c+\frac{\partial^2\bar{u}_z}{\partial x^2}c^2,\text{ with } c=\frac{\partial x}{\partial t} \tag{4}$$

Moreover, the moving system was supposed to be described by equivalent distributed loads and masses acting over the girder profile.

With respect to a moving reference system, from the left end of the bridge, and to an eccentricity distance *e* of the moving load with respect to the centroid of the cross section, the mass and loading functions during the external load advance, can be written by the following expressions:

$$\rho=\lambda H\left(x_1+L_p-ct\right)H\left(ct-x_1\right) \tag{5}$$

$$f=pH\left(ct-X\right)H\left(X+L_p-ct\right) \tag{6}$$

$$\rho_0=\lambda_0 H\left(x_1+L_p-ct\right)H\left(ct-x_1\right) \tag{7}$$

$$m=p\cdot e\, H\left(ct-x_1\right)H\left(x_1+L_p-ct\right) \tag{8}$$

where $H(.)$ is the Heaviside function, L_p is the length of the moving loads, x_1 is the referential coordinate located at the left end girder cross section, (λ, p) are the per unit length mass and self-weight loads, respectively, and λ_0 represents the torsional distributed polar mass moment produced by the external loading. The dynamic equilibrium equations were derived in explicit form, consistently with a variational approach, in which both internal and external works were evaluated by means of the following relationship:

$$\begin{aligned}&\sum_c\int\left(N\delta\varepsilon_n+M_x\delta\chi_x+M_y\delta\chi_y+M_t\delta\theta_x\right)dL+\\&\sum_c\int\mu\ddot{\underset{\sim}{u}}\delta\underset{\sim}{u}dL+\sum_c\int\mu_0\ddot{\underset{\sim}{u}}\delta\underset{\sim}{u}dL=\sum_c\int\underset{\sim}{g}_G\delta\underset{\sim}{u}dL+\\&\sum_c\underset{\sim}{F}\delta\underset{\sim}{u}dL+\sum_c\int\rho\left(\ddot{\bar{u}}_z+2c\dot{\bar{u}}_z+c^2\bar{u}''_z\right)\delta\bar{u}_z dL+\\&\sum_c\int\dot{\rho}\dot{\bar{u}}_z\delta\bar{u}_z dL\end{aligned} \tag{9}$$

where (N, M_x, M_y, M_t) are the internal stress resultants, (ε_n, χ_x, χ_y, θ) are the corresponding generalized beam strains, (μ, μ_0) are mass moment and polar mass moment of the girder, g_c is the self-weight load of the girder and F is reaction force vector.

2.3 Corrosion Mechanism Formulation

With reference to the structural bridge scheme reported in Fig.1, it was assumed that the cable system was composed of undamaged elements and a fixed number of elements which were affected by an internal cable damage mechanism. The cable corrosion mechanism was formulated, consistently with a Continuous Damage Mechanics approach in which cable deterioration results in the reduction in cable cross-sectional area [12-13].

Therefore, denoting with A_0 the cross-sectional area of the cable in a perfect state, and with A^* the reduced area due to cable corrosion, the effective area A_{eff} is defined as:

$$A_{eff}=A_0-A^* \tag{10}$$

Then the corresponding corrosion ratio can be defined in the form:

$$D=\frac{A_{eff}}{A_0}=\frac{A_0-A^*}{A_0} \tag{11}$$

Consistently with CDM, the effective stress σ_{eff} is defined as the ratio between the tensile force (T) and the effective area:

$$\sigma_{eff}=\frac{T}{A_{eff}} \tag{12}$$

Since $\sigma A_0=\sigma_{eff}A_{eff}$ and according to Eq. (11) we obtain:

$$\sigma_{eff}=\frac{\sigma}{1-D} \tag{13}$$

By introducing Lemaitre's equivalent-strain principle, the following expression concerning the stresses in the corroded or the effective configurations can be derived: (Fig. 2).

$$\varepsilon=\frac{\sigma}{E_{eff}}=\frac{\sigma_{eff}}{E}=\frac{\sigma}{(1-D)E} \tag{14}$$

Finally, on the basis of Eq. (13) and Eq.(14), the effective modulus of elasticity E_{eff} for corroded cable can be defined by the following relationship:

$$E_{eff}=\frac{A_{eff}}{A_0}E \quad (15)$$

3. Finite element implementation

Governing equations given by Eq. (1) and Eq. (9) introduce a nonlinear set of equations, which were solved numerically, using COMSOL Multiphysics TM version 4.2a. Fig. 2. Finite element expressions were written starting from the weak form, introducing isoparametric shape functions (ζ_i, ξ_i) to represent cable and girder variables as:

$$\begin{aligned}\underset{\sim}{u}_C(r,t)&=\sum_{i=1}^{n}\zeta_i(\underset{\sim}{r})\,\underset{\sim}{u}_{iC}(t)\\ \underset{\sim}{u}_G(r,t)&=\sum_{i=1}^{n}\xi_i(\underset{\sim}{r})\,\underset{\sim}{u}_{iG}(t)\end{aligned} \quad (16)$$

Where n represents the number of nodes of the master finite element. In particular, Lagrange interpolation functions were adopted to analyze the behavior of the cable system, whereas for girder elements based on EB formulation Hermit cubic interpolation functions were employed.

Substituting Eq. (16) in the governing equations, given by Eq. (1) and Eq. (9), the following discrete equilibrium equations were obtained:

$$\begin{aligned}&\sum_{i=1}^{n}\left[\underset{\sim}{M}_i+\underset{\sim}{N}_i^1\right]\ddot{\underset{\sim}{U}}_i+\sum_{i=1}^{n}\underset{\sim}{N}_i^2\underset{\sim}{U}_i+\\ &\sum_{i=1}^{n}\left(\underset{\sim}{K}_i+\underset{\sim}{N}_i^3\right)\underset{\sim}{U}_i=\sum_{i=1}^{n}\underset{\sim}{P}_i\end{aligned} \quad (17)$$

where M_i is the mass matrix, K is the stiffness matrix, P_i is the external load vector and (N^1_i, N^2_i, N^3_i) are non-standard matrix obtained from the coupling effects produced by the interaction forces between moving loads and bridge motion. In order to solve the nonlinear algebraic equations an implicit time integration scheme based on a variable step-size backward differentiation formula (BDF) was adopted. Moreover, during the time integration, due to the fast speeds of the moving loads, a small time step size was utilized, which typically, no more than 1/10 of the fundamental period of vibration of the structure.

4. Numerical results and conclusions

Results are presented for cable supported bridges based on both suspension and cable-stayed configurations, adopting similar properties for the main constituents of the bridge structures, i.e. girder, cable system and pylons. Mechanical characteristics concerning cable-stayed and suspension bridges, reported in Fig.1, are opportunely selected consistently to typical values utilized in several bridge applications and mainly derived from both structural and economic reasons.

The analyses are reported for bridge structures with different damage mechanisms in the cable system Fig.1. At first, the effect of the damage mechanisms is analyzed in the suspension bridge, in which two different damage scenarios, with *D=0.5*, were considered (Fig.s 1a,1b). It is worth noting that the damage was assumed only in one of the two cables planes, precisely on the side where the load runs. Furthermore, the analyzes were carried out under the assumption that corrosion mechanisms were

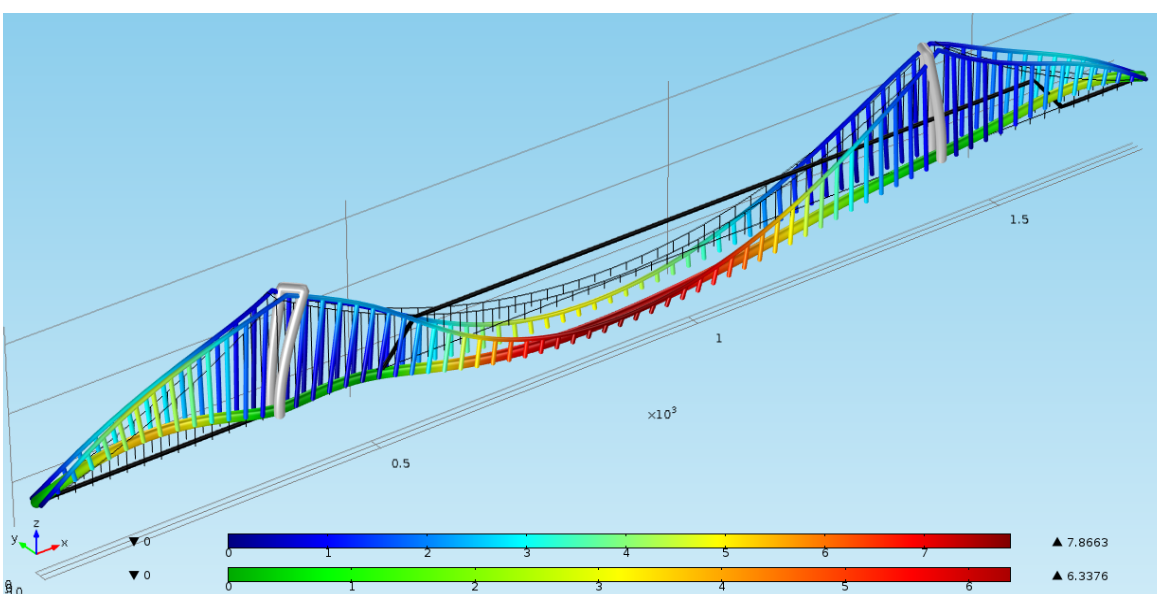

Figure 2. Suspended bridge: Comsol Multiphysics 4.2a model

present before the transit of the moving load.

The presence of corroded cables involves a variation of the zero configuration obtained without damage. The results are presented in terms of time histories of typical cinematic and stress design variables, comparing the dynamic behavior between cable-stayed bridges and suspension bridges in the cases of damage and undamaged bridge configurations.

In order to study the influence of the speed of the moving load on the bridge behavior, the hypothesized damage scenarios were analyzed for two different reference speeds.

For the sake of brevity, results are presented in terms of the midspan vertical displacement only. Results concerning the behavior of suspension bridges, in terms of time histories of the midspan displacement are reported in Fig 3.

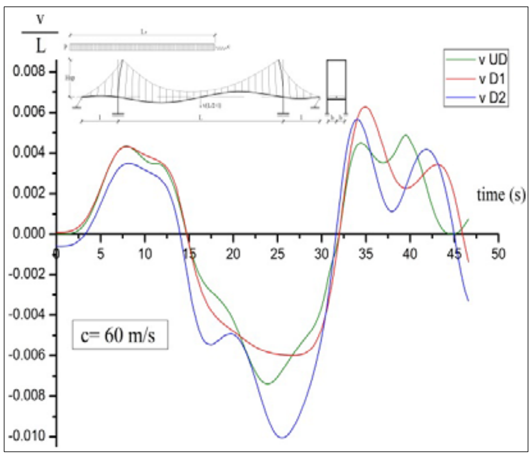

Figure 3. Suspended bridge: Time History of the midspan displacement

The analyses show that bridge deformations are quite dependent for the assumed damage scenario. As a matter of fact, the effects concerning the presence of damage produce with respect to the undamaged bridge configuration a maximum percentage increment of the maximum displacement equal to 26.66. In the framework of cable-stayed bridges, the analyses, reported in Fig.s 4,5, denote that the presence of a partial damage in the anchor cable is able to produce high amplifications of the bridge displacements with respect to the undamaged configuration.

As a matter of fact, the observed maximum percentage increment of the midspan displacements are equal to 67.51 (Tab. 2)

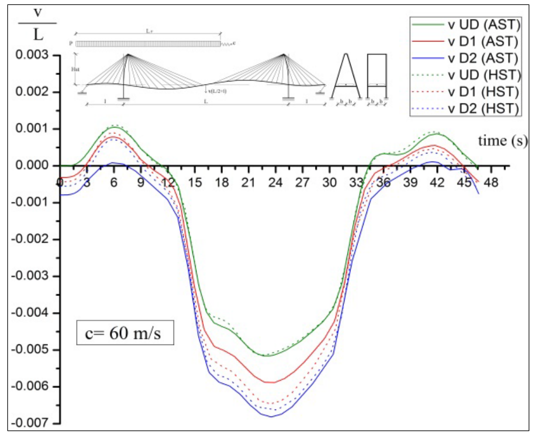

Figure 4. Cable-stayed bridges: Time History of the midspan displacement – c = 60 m/s

	UD	D1	D2	% Amp. D1	% Amp. D2
H_{shaped}	5.13	5.67	6.92	***10.45***	***34.70***
A_{shaped}	5.16	5.72	7.05	***10.91***	***36.66***

Table 1. Cable-stayed bridges: Maximum values of the midspan displacement and amplification percentage – c = 60 m/s

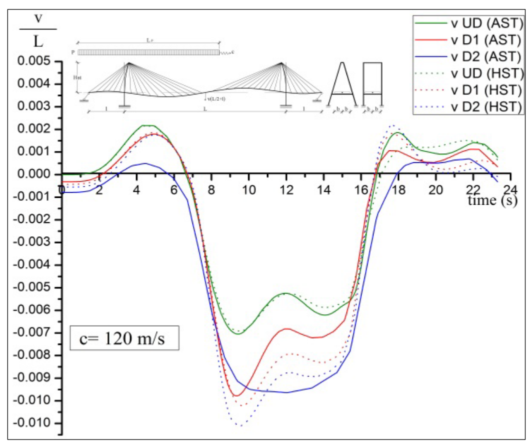

Figure 5. Cable-stayed bridges: Time History of the midspan displacement – c = 120 m/s

	UD	D1	D2	% Amp. D1	% Amp. D2
H_{shaped}	6.63	8.09	11.1	***22.15***	***67.51***
A_{shaped}	6.82	8.16	9.64	***19.80***	***41.43***

Table 2. Cable-stayed bridges: Maximum values of the midspan displacement and amplification percentage – c = 120 m/s

Finally, in Fig.s 6,7, results concerning both cable-stayed and suspension bridge scheme reported in terms of damage scenarios, bridge characteristics and moving loads transit speeds.

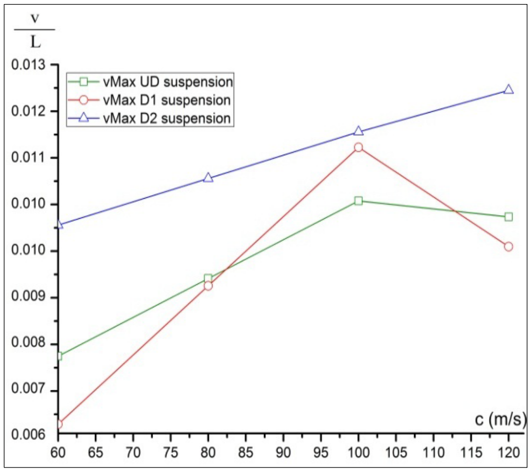

Figure 6. Suspended bridge: Maximum vertical midspan displacement - influence of the speed

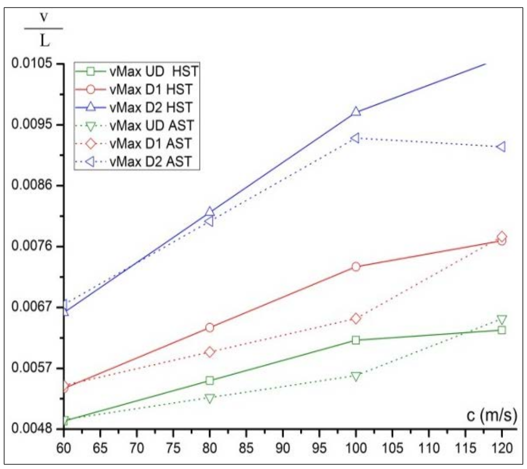

Figure 7. Cable-stayed bridge: Maximum vertical midspan displacement - influence of the speed

The comparison show how cable-stayed bridges are much more affected by the presence of the damage and the transit speed of the moving loads, since larger values of the bridge displacements with respect to the undamaged configuration are observed.

5. References

1. Gimsing N., *Cable supported bridge – Concept and design*, John Wiley & Sons, New York.
2. Nakamura S., Suzumura K., Hydrogen embrittlement and corrosion fatigue of corroded bridge wires, *Journal of Constructional Steel Research*, **65**, 269-277 (2009).
3. Nakamura S., Suzumara K., Tarui T., Mechanical Prpperties and Remaining Strength of Corroded Bridge Wires, *Structural Engineering International*, **1/2004**, 50-54 (2003).
4. Barney T., Martin Jr., Evolution of Parallel Wire Cable Condition Assessment – A case study, 24th US - *Japan Bridge Engineering Workshop*, 121-134 (2008).
5. Zhang H., Xie X., Dynamic responses of cable-stayed bridges to vehicular loading including the effects of the local vibration of cables. *Journal of Zhejiang University: Science A.*, **12 (8)**, 593-604 (2011).
6. Chatterjee P. K., Datta T. K., Surana C. S., Vibration of cable-stayed bridges under moving vehicles, Structural Engineering International, 4, 116-121 (1994).
7. Bruno D., Greco F., Lonetti P., Dynamic impact analysis of long span cable-stayed bridges under moving loads. *Engineering Structures*, **30**, 1160-1177 (2008).
8. Bruno D., Greco F., Lonetti P., A parametric study on the dynamic behaviour of combined cable-stayed and suspension bridges under moving loads, *International Journal for Computational Methods in Engineering Science & Mechanics*, **10**, 243-258 (2009).
9. Bruno D., Greco F., Lonetti P., Pascuzzo A., Dynamic analysis of long span cable-stayed bridge under the action of moving loads, International conference IBSBI 2011 - *Innovations on bridge and soil-bridge interaction*, 513-520 (2011).
10. Lepidi M., Gattulli V., Vestroni F., Static and dynamic response of elastic suspended cable with damage, *Internationa journal of solids and structures*, **44**, 8194-8212 (2007).
11. Materazzi A. L., Ubertini F., Eigenproperties of suspension bridges with damage, *Journal of sound and vibration*, **330**, 6420-6434 (2011).
12. Huang J., Wang R., Tang T., Formulation for cable state of existing cable-stayed bridge, Proceedings of the 26th Southern *Africa Transport Conference (SATC 2007)*, 745-751 (2007).
13. Lemaitre J., Desmorat R., *Engineering damage mechanics*, Springer Berlin Heidelberg, New York.